UNIVERSITY OF MARYLAND

INSTITUTE FOR MOLECULAR PHYSICS

SOME ASPECTS OF THE QUANTAL AND SEMICLASSICAL CALCULATION OF PHASE SHIFTS AND CROSS SECTIONS FOR MOLECULAR SCATTERING AND TRANSPORT

R. J. Munn, E. A. Mason, and Francis J. Smith

IMP-NASA-38

July 31, 1964

SOME ASPECTS OF THE QUANTAL AND SEMICLASSICAL CALCULATION OF PHASE SHIFTS AND CROSS SECTIONS FOR MOLECULAR SCATTERING AND TRANSPORT*

R. J. Munn,† E. A. Mason, and F. J. Smith‡
Institute for Molecular Physics, University of Maryland
College Park, Maryland

ABSTRACT

A critical study is made of the JWKB approximation for phase shifts by comparison of the approximate phases with those calculated by numerical solution of the radial wave equation. A region of $E - \ell - \Lambda^*$ space is mapped out for the Lennard-Jones (12-6) potential in which the JWKB approximation is unsatisfactory. Reasons for the failure of the JWKB approximation are noted, and a simple but effective method of predicting the region of $E - \ell - \Lambda^*$ space where failure occurs is suggested. The study is continued by a comparison of the quantal and semiclassical transport and total cross sections.

---

* Supported in part by the National Aeronautics and Space Administration (Grant NsG-5-59).

† Harkness Fellow of the Commonwealth Fund, 1963-1964; on leave from the Department of Physical Chemistry, The University, Bristol, England.

‡ On leave from the Department of Applied Mathematics, Queen's University of Belfast, Northern Ireland.

It is shown that the JWKB transport cross sections are of limited practical value and that the semiclassical total cross sections are useful only at high values of E and low values of Λ^*. Particular attention is centered on features associated with classical orbiting and with semiclassical rainbow and glory scattering. An apparent sign change in the quantum corrections for the viscosity cross section found by de Boer and Bird is shown to be an artifact caused by the neglect of the attractive part of the interaction potential. Finally, small-angle quantal differential cross sections for a repulsive r^{-12} potential are compared with some recent semiclassical calculations. The behavior as $\exp(-c\chi^2)$ at small angles is found to be valid to larger angles than previously thought.

I. INTRODUCTION

Elastic collisions between atoms and molecules are described by the laws of quantum mechanics. A complete quantal phase-shift calculation of scattering and transport cross-sections, however, can be very laborious, especially when large numbers of phase shifts are required; valid approximations are therefore often made. Two main levels of approximation exist: (1) the phase shifts can be approximated instead of being calculated by direct numerical integration of the radial wave equation, and (2) the various summations of the phase shifts to produce cross sections can also be approximated. When enough such approximations are made, the results reduce to those of a purely classical calculation; there are, however, intermediate stages between the pure quantal and the pure classical calculations.

The object of this paper is to establish the domain of validity of the "semiclassical" and classical approximations for some atomic and molecular collisions, and to point out some features that arise in cross sections when the scattering potential has both attractive and repulsive branches. These features are connected with the classical orbiting collisions, and with scattering patterns known as glories and rainbows from the analogous optical phenomena.[1] Attention is centered on the total scattering cross section and on the transport cross sections for diffusion and viscosity, and only a few

remarks on the differential scattering cross sections are made. Although the phenomena discussed are considered to be quite general, detailed numerical calculations are for the most part restricted to the Lennard-Jones (12-6) potential.

Comparison is also made with several recent studies of molecular scattering.[2-5] The previous calculations turn out to be restricted to parameter values for which the semi-classical (JWKB) approximation is quite accurate, and do not really come very close to the truly quantal regions. Some of their conclusions must therefore be treated with reservation.

II. GENERAL FORMULAS

In the phase-shift formulation, the differential scattering cross section for central forces is

$$\sigma(\chi) = \frac{1}{4k^2} \left| \sum_{\ell} (2\ell+1) \left[\exp(2i\delta_\ell)-1 \right] P_\ell(\cos \chi) \right|^2, \quad (1)$$

where $k = \mu v/\hbar$ is the wave number of relative motion, χ is the angle of deflection of the relative velocity vector, δ_ℓ is the phase shift for angular-momentum quantum number ℓ, and $P_\ell(\cos \chi)$ is a Legendre polynomial in $\cos \chi$. The total scattering cross section S and the transport cross sections $S^{(n)}$ are defined in terms of $\sigma(\chi)$ by

$$S = 2\pi \int_0^{\pi} \sigma(\chi) \sin \chi \, d\chi , \quad (2)$$

$$S^{(n)} = 2\pi \int_0^{\pi} (1 - \cos^n \chi)\sigma(\chi) \sin \chi \, d\chi. \tag{3}$$

When $\sigma(\chi)$ is substituted in Eqs. (2) and (3), the integrations can be carried out to yield[6]

$$S = \frac{4\pi}{k^2} \sum_{\ell} (2\ell + 1) \sin^2 \delta_{\ell}, \tag{4}$$

$$S^{(1)} = \frac{4\pi}{k^2} \sum_{\ell} (\ell + 1) \sin^2(\delta_{\ell+1} - \delta_{\ell}) , \tag{5}$$

$$S^{(2)} = \frac{4\pi}{k^2} \sum_{\ell} \frac{(\ell+1)(\ell+2)}{(2\ell+3)} \sin^2 (\delta_{\ell+2} - \delta_{\ell}) , \tag{6}$$

which are the usual starting points for numerical calculations. The summations run over all integral values of ℓ from 0 to ∞ for distinguishable particles, but only over even or odd integral values of ℓ for indistinguishable particles. The diffusion cross section $S^{(1)}$ must always refer to distinguishable particles or else it refers to a nonobservable process.

Accurate numerical values of the phase shifts δ_{ℓ} can be determined by solving the radial wave equation of the relative motion either analytically or numerically. The former approach is limited to some very simple scattering potentials; the latter procedure is nearly always feasible for "physically reasonable" potentials but it is laborious and time-consuming. The approximation that is usually used for atomic and molecular

scattering is often called semiclassical, a term which we shall use to mean that the summations over phase shifts are replaced by integrations and that the phase shifts δ_ℓ are calculated using the JWKB approximation with the Langer modification of replacing $\ell(\ell+1)$ by $(\ell+\frac{1}{2})^2$ in the centrifugal term. We write this approximation as

$$\delta_\ell \approx \delta(b) = k\int_{r_o}^{\infty}\left[1 - (b/r)^2 - (\varphi(r)/E)\right]^{\frac{1}{2}} dr - k\int_{b}^{\infty}\left[1 - (b/r)^2\right]^{\frac{1}{2}} dr, \tag{7}$$

where $\varphi(r)$ is the scattering potential and

$$b = (\ell+\tfrac{1}{2})/k \quad , \quad E = \tfrac{1}{2}\mu v^2. \tag{8}$$

The lower limits of the integrals are the outermost zeroes of their integrands; r_o corresponds to the classical distance of closest approach and b to the classical impact parameter. A more general treatment[7] shows that in cases where there is more than one zero of the first integrand in Eq.(7), the result still holds in the same form but the integration extends over all ranges for which the integrand is real. We do not use this extension in order to preserve the important semiclassical relation between the phase shifts and the classical deflection angle,

$$\chi(b) = \frac{2}{k}\frac{d\delta}{db} = 2\frac{d\delta_\ell}{d\ell} \quad . \tag{9}$$

For small phase shifts the JWKB approximation becomes equivalent to the Born approximation.

Our first task will be to examine the range of validity of the JWKB phase-shift approximation, and then to consider the cross-section calculations.

III. PHASE SHIFT CALCULATIONS

All phase shift calculations were performed by numerical integration with an IBM 7090. The numerical methods used for the JWKB integration have been described elsewhere,[8] and the numerical methods used for the integration of the radial wave equation are described in the Appendix. Although nothing new in principle is involved in these numerical methods, the programs ran appreciably faster than those previously described[2-5] with no loss of accuracy. The potential used was the Lennard-Jones (12-6),

$$\varphi(r) = 4\epsilon \left[(\sigma/r)^{12} - (\sigma/r)^{6} \right], \qquad (10)$$

where ϵ is the well depth and $\varphi(\sigma) = 0$. The quantum effects are characterized by the de Boer parameter,

$$\Lambda^* = h/\sigma(2\mu\epsilon)^{\frac{1}{2}}, \qquad 11)$$

where h is Planck's constant and μ the reduced mass of the system. Λ^* is the de Broglie wavelength of the colliding system in units of σ for an energy of $E = \epsilon$, or the thermal de Broglie

wavelength for a temperature of $T = \epsilon/k$. The value of Λ^* for light molecules ranges from 1.0 for tritium to slightly greater than 3.0 for helium-3. The values for "classical"molecules lie in the range 0 to 1.0; for example, Λ^* is 0.59 for neon. Earlier calculations[2,3] have concentrated on cases corresponding to $\Lambda^* = 0.56$, and so have not encountered many of the striking quantum effects obtained by varying Λ^*.

A comparison of the quantal and JWKB phase shifts shows that there is always a region in which the JWKB approximation is poor, and that this region grows in extent as Λ^* increases. An illustration of the type of failure encountered is shown in Fig. 1, where δ_ℓ is plotted as a function of E/ϵ for values of $\ell = 5$, 6, and 7 and $\Lambda^* = 1.0$. A fixed value of ℓ corresponds to a fixed value of the angular momentum. The vertical arrows mark the energies for which classical orbiting occurs; the failure of the JWKB phase-shift approximation is particularly obvious at energies close to the orbiting energies. It is easy to understand why this is so: for energies below the orbiting energy, penetration of the centrifugal barrier by tunneling occurs, and since the JWKB approximation contains no provision for tunneling, the approximation is poor. For energies above the orbiting energy, the incoming wave is partially reflected by the centrifugal barrier and the JWKB approximation is again rather poor. Thus at given values of ℓ and Λ^* there may be a range of energies for which the JWKB approximation is unsatisfactory.

The parameter values for which the JWKB approximation is

unsatisfactory can be represented as a region in the E-$\underline{\ell}$ plane for each value of Λ^*. The regions for different Λ^* can be made to exhibit a clear family resemblance by using as one coordinate not $\underline{\ell}$ but $\Lambda^*(\ell+\frac{1}{2})$, which is proportional to the angular momentum $b(2\mu E)^{\frac{1}{2}}$, as follows:

$$\Lambda^* \ (\ell + \tfrac{1}{2}) \ = 2\,\pi\,(b/\sigma)\,(E/\epsilon)^{\frac{1}{2}} \ . \qquad (12)$$

Such a plot is shown in Fig. 2, constructed with the criterion that the JWKB approximation is unsatisfactory when the discrepancy with the quantal phase shifts is greater than 0.05 rad. Other choices of criteria would narrow or widen the regions shown, but would not change the overall picture. The choice of variable given by Eq.(12) causes the regions to coincide along one edge. This edge runs very close to the curve which defines classical orbiting, and in fact continues beyond it near the curve which defines rainbow scattering.

It is not surprising that the JWKB approximation fails in the vicinity of classical orbiting, because of barrier tunneling and partial reflection, but it is more surprising that it also fails at energies $E/\epsilon > 0.8$, where no centrifugal barrier exists. However, the reason is not hard to find, and can be understood by reference to Fig. 3, where two effective potential curves,

$$\varphi_{\text{eff}}\ (r)/\epsilon \ = 4(\sigma/r)^{12} - 4(\sigma/r)^{6} + \left[(E/\epsilon)\,(b/\sigma)^{2}\right](\sigma/r)^{2}, \qquad (13)$$

are shown, one with a barrier and one without. The φ_{eff} curve without the barrier retains a trace of the barrier in the form of a "kink" in the curve. When the kink is rather abrupt, it can cause a reflected wave to be set up which is not taken into account in the JWKB approximation. This failure in the JWKB formulation disappears only when the angular momentum becomes still greater and the kink straightens out or when E is so high that the kink appears unimportant in comparison. It is surprising how high E must be before this occurs.

An important practical question is how to predict the regions, shown in Fig. 2, where the quantal calculations must be used. It is little help to know that such regions do exist if the only way to find them is by direct comparison of JWKB and quantal phase shifts. It is clear that a reasonable estimate of the low-energy edges of the regions is available from a knowledge of the curve of classical orbiting and rainbow scattering; the problem is therefore to predict the high-energy edges. A satisfactory prediction can be obtained from a rough analysis based on the idea that the high-energy edges indicate where partial reflection by the centrifugal barrier or the kink becomes negligible. All we really need to know is how the edge energy varies with Λ^*, for which purpose a rectangular barrier of height φ_o and width $\underline{a}$ may serve as a sufficient mimic of the complicated real barrier. The reflection coefficient R of such a barrier for $E > \varphi_o$ is[9]

$$R = \left[1 + \frac{4E(E-\varphi_o)}{\varphi_o^2 \sin^2 \alpha a} \right]^{-1} , \tag{14}$$

where

$$\alpha = \left[2\mu (E-\varphi_o) \right]^{\frac{1}{2}} / \hbar . \tag{15}$$

As E increases above φ_o, R decreases asymptotically to zero, but with an oscillating component due to the sharp corners of the square barrier. After the first zero of R, which occurs for $\alpha a = \pi$, the value of R is always less than 0.1, and after the second zero at $\alpha a = 2\pi$, the value of R remains less than 0.02. So we can expect reflections to cause little trouble when αa becomes greater than some constant, say roughly 2π, that is if

$$a \left[2\mu (E-\varphi_o) \right]^{\frac{1}{2}} \gtrsim h. \tag{16}$$

Substituting for Λ^* and taking $E >> \varphi_o$, we find this condition becomes

$$E/\epsilon \geq \text{constant} \times (\Lambda^*)^2. \tag{17}$$

Thus a plot of the value of the edge energy vs. $(\Lambda^*)^2$ should be approximately a straight line through the origin. This conclusion is tested in Fig. 4, and shown to hold with surprising accuracy both for a point near the bottom of the edge and for the uppermost regions of the edges. That is, the relation holds even when extrapolated into the region where the barrier has degenerated into a kink.

From Figs. 2 and 4 we can therefore predict with some confidence the regions where quantal calculations of phase shifts should be made for the Lennard-Jones (12-6) potential. The regions will probably be somewhat different for other forms of potential, but Figs. 2 and 4 indicate how the boundaries of the regions can be located with the minimum of computational effort, using the orbiting edge and Eq.(17). The regions always enclose the orbiting curve, but as Λ^* decreases they draw closer and eventually become just a thin strip on either side of the orbiting curve. Thus for small values of Λ^* the JWKB approximation is accurate except near classical orbiting.

Figure 2 also affords an explanation of several recent conclusions about phase shifts for the 12-6 potential. For instance, Bernstein[2] found that his quantal phase shifts were remarkably well correlated in terms of reduced parameters suggested by a semiclassical analysis. The reason for this success can now be seen to lie in the fact that Bernstein confined his calculations to values of Λ^* less than unity. Had he compared his reduced phase shifts with the existing quantal calculations for larger Λ^*, carried out in a study of helium for instance,[10] he would have found very large discrepancies. As another example, the pattern of agreement and disagreement found by Choi and Ross[11] between Bernstein's quantal calculations and their second-order WKB calculations is nicely correlated by Fig. 4. The success of Marchi and Mueller[3] with the JWKB approximation is due to their fortuitous avoidance, for the most part, of the regions shown in Fig. 4.

This is largely due to their using $\Lambda^* = 0.56$.

A few comments on the behavior of the phase shifts in the region of classical orbiting are in order. Here the phase shift changes rapidly over a very small range of $\underline{b}$ at fixed E, and the impression is often obtained that there is a sharp discontinuity in both value and slope of the phase shift at the orbiting point.[1b,2,3,12,13] While it is true that some kinds of primitive semiclassical calculations do give such behavior, the JWKB phase shifts (in the sense used here) are much smoother, although exhibiting infinite slope and a discontinuity at the orbiting point, as is shown schematically in Fig. 5 (see also Fig. 3 of reference 1a). It is clear from the semiclassical relation between δ and χ, Eq.(9), that δ cannot have a finite slope at orbiting, or else χ would exhibit a cusp instead of a singularity. The quantal phases are everywhere discontinuous, strictly speaking, since $\underline{\ell}$ takes on only integral values. However, if we consider $\underline{\ell}$ as a continuous variable for purposes of mathematical discussion, then δ is continuous across the orbiting point, as shown in Fig. 5.

Figure 5 further shows that JWKB phase shift differences can be more accurate than the phase shifts themselves because the JWKB phase-shift curve runs very nearly parallel to the quantal curve over a large range. One consequence of this is that transport cross sections, which involve only differences of phase shifts, may be more accurate than differential or total scattering cross sections when calculated with JWKB phase shifts.

IV. CROSS SECTION CALCULATIONS

Relations among Quantal, Semiclassical, and Classical Cross Sections

We can now apply the results of the phase-shift analysis to the calculation of various cross sections, to see the effects of the quantum deviations. Ford and Wheeler[1a] have previously pointed out that there will always be regions where the quantal and classical differential cross sections differ by a large amount. Whether or not these deviations propagate into the transport cross sections depends on the angle at which the deviations in $\sigma(\chi)$ occur. The well-known divergence in the classical $\sigma(\chi)$ at $\chi = 0$ does not propagate into the transport cross sections because of the $(1-\cos^n\chi)$ weighting factors. That the divergence at the rainbow angle χ_r, where $\sigma(\chi_r)$ diverges[1a,14] as $\hbar^{-1/3}$, also does not propagate into the transport cross sections is more surprising, since χ_r can have any value for the 12-6 potential, depending on the energy. The fact is not obvious from the expression for $S^{(n)}$ in terms of $\sigma(\chi)$ given by Eq. (3), but follows easily from the expressions for $S^{(n)}$ in terms of phase shifts given by Eqs. (5) and (6). Passing to the semiclassical limit, we replace the summations over ℓ by integrations over b and the phase-shift differences by $d\delta_\ell/d\ell$, which is related to χ according to Eq. (9), and obtain

$$S^{(1)} = 4\pi \int_0^\infty \sin^2(\chi/2)\, b\, db = 2\pi \int_0^\infty (1 - \cos\chi)\, b db, \qquad (18)$$

$$S^{(2)} = 2\pi \int_0^\infty \sin^2\chi \; bdb = 2\pi \int_0^\infty (1-\cos^2\chi)\, bdb. \qquad (19)$$

These are exactly the classical expressions obtainable from Eq. (3) by the classical substitution, $\sigma(\chi)\ \sin\chi\ d\chi = bdb$. Thus the ever-present divergence in $\sigma(\chi)$ around χ_r is without influence in the semiclassical limit.

The fact that a consistent semiclassical approximation of the transport cross sections, including replacement of the summations by integrations, leads to the exact classical result is apparently not as well known as it deserves to be, although it has certainly been pointed out previously.[6,13] Since this particular semiclassical approximation turns out to be in fact completely classical, it is perhaps better to use the term "JWKB transport cross sections" to mean those that are evaluated with JWKB phase shifts, but with the summations over ℓ not converted to integrations. Unless only a few phase shifts contribute to the summation, however, such JWKB cross sections will differ but little from completely classical cross sections (except in orbiting regions as explained later).

Furthermore, since there are always situations (large Λ^* and low E) where quantum deviations are large for the transport cross sections, we shall expect that in such cases the JWKB approximation will be little better than the pure classical approximation. That this is indeed the case is shown in Fig. 6, where the percentage deviations of the classical and JWKB $S^{(1)}$ from the correct quantal results are shown as a function of energy

for $\Lambda^* = 1.0$ and 2.67.

The conclusion to be drawn from Fig. 6 is that it is seldom worthwhile to bother with a JWKB approximation to $S^{(n)}$, and that a numerically accurate classical calculation is likely to be better than a numerically cruder JWKB calculation with an apparently better theoretical pedigree.[13,15] This is of course not true for the total scattering cross section S, for which the classical approximation always fails completely, but for which the JWKB approximation may be quite satisfactory provided Λ^* is not too large nor E too small. This is shown in Fig. 7 where the percentage deviations of the JWKB S from the correct quantal S are shown as a function of energy for several values of Λ^*.

Wood and Curtiss[16] have given the first two correction terms for the quantum deviations of $S^{(1)}$ and $S^{(2)}$, which are proportional to $\hbar^2$ and $\hbar^4$. These arise in part from a higher-order WKB expansion for the phase shifts,[7] and in part from Euler-Maclaurin corrections which arise when the summations are approximated by integrations. No numerical results have yet been reported, only general formulas, and it remains to be seen how fast the convergence will be in actual computations. It is conceivable that a combination of quantal and JWKB phase shifts, based on Fig. 2, could be calculated and combined to form cross sections with better accuracy for a comparable amount of labor than can be obtained from use of the series in $\hbar^2$. The question is worth further investigation.

Regardless of which method may be the most efficient for numerical computation, the present results can be used to throw some light on an interesting peculiarity in the quantum deviations of the viscosity of He^4 at low and high temperatures, or what is the same thing, the quantum deviations of $S^{(2)}$ at low and high energies. At low energies, de Boer[17] found that the quantal $S^{(2)}$ was smaller than the classical $S^{(2)}$ for the 12-6 potential with parameters corresponding to He^4. He was not able to go to higher energies at that time because of limited computing facilities. Some years later de Boer and Bird[18] carried out a semiclassical expansion in powers of $\hbar^2$ (the later work of Wood and Curtiss is a revision and extension of this). However, they limited their numerical calculations to an r^{-12} repulsive potential, believing that the attractive r^{-6} term of the 12-6 potential would be unimportant at high energies. For an r^{-12} repulsive potential they found the quantal $S^{(2)}$ to be <u>larger</u> than the classical $S^{(2)}$. They therefore concluded that the quantal and classical curves crossed at roughly $E/\epsilon=4$. The actual situation is shown in Fig. 8, where the quantal and classical $S^{(2)}$ for the 12-6 potential are shown together with the quantal $S^{(2)}$ for the corresponding r^{-12} potential, $\varphi = 4\epsilon(\sigma/r)^{12}$. It is seen that the quantal $S^{(2)}$ lies below the classical $S^{(2)}$ at <u>all</u> energies for the 12-6 potential, and that the apparent cross-over was an artifact caused by dropping the attractive term in the potential.

A semiclassical expansion of $\sigma(\chi)$ at small angles in powers of $\hbar^2$ has also been given recently.[14,19] These quantum deviations arise primarily from improvements to the stationary phase method for evaluating the semiclassical differential cross section.[1a] Other quantum deviations, due to higher terms in the Euler-Maclaurin summation formula and to higher-order WKB approximations, are much smaller in this region. However, if the expression for $\sigma(\chi)$ in powers of $\hbar^2$ is used in Eq.(3) to evaluate $S^{(n)}$, the stationary-phase small-angle quantum corrections are greatly attenuated by the $(1-\cos^n\chi)$ weighting factors and no longer dominate the other quantum corrections in the final expressions for $S^{(n)}$. They are, in fact, of comparable magnitude, as Wood and Curtiss[16] have shown. In other words, the expressions given for the quantum deviations of $\sigma(\chi)$ at small angles[14,19] give only half the full[16] quantum corrections to $S^{(n)}$. Indeed, the approach to $S^{(n)}$ through $\sigma(\chi)$ and Eq.(3) is very poor for computational purposes, and the direct expressions in terms of phase shifts, Eqs.(5) and (6), are to be preferred.

Orbiting and Rainbow Effects

We now consider the effects of classical orbiting and rainbow scattering on the computation of cross sections. Some of these effects are already known, but their detailed influences on numerical computations have often been overlooked. Consider first the JWKB approximations to the cross sections — that is,

the JWKB phase shifts and summations over $\underline{\ell}$. A plot of δ_ℓ vs. $\underline{\ell}$ at constant E looks very much like Fig. 5, and as E is increased the vertical portion of the curve (corresponding to classical orbiting) moves to higher ℓ values. As the steep "front" crosses each integral value of $\underline{\ell}$, the phase shift for that $\underline{\ell}$ takes a sudden jump and this may be reflected as a sharp jump in the cross sections at that energy. (Of course the exact effect on the cross section depends on the height of the front. If it is approximately $s\pi$ then no jump is observed; see Fig. 9 where the ℓ=3 jump is missing for this reason.) The variation of the δ_ℓ and of the cross sections is smooth as E increases further, until the front reaches the next integral value of $\underline{\ell}$, when another jump occurs. The result is a sawtooth appearance (with some teeth missing) to the cross sections as a function of energy. The sawteeth are generally more noticeable for the $S^{(n)}$ than for the S, since the former involve phase shift differences.

The orbiting sawteeth persist until E is so high that orbiting is no longer possible, and only rainbow scattering occurs. Then the front of the δ_ℓ vs. $\underline{\ell}$ curve becomes less steep and there is only an undulation in the cross section. These gentle undulations die out rapidly as the energy increases further and the δ_ℓ vs. $\underline{\ell}$ curve becomes still more slowly-varying.

The effect of a correct quantal calculation in the classical orbiting region is usually to make the fronts of the δ_ℓ vs. $\underline{\ell}$ curves less steep, although the front may sometimes

tunnel through the orbiting region with little change in shape, somewhat as shown in Fig.1. The general effect is thus to round off the tips of the orbiting sawteeth and reduce their magnitude and, to some extent, their location (this is very severe if Λ^* is large). The appearance is as if the orbiting sawteeth were largely converted into rainbow undulations, as is indeed the case, since quantal barrier penetration converts classical orbiting into semiclassical rainbow scattering.[1a] However, some of the JWKB sawteeth are converted into sharp spikes, and an occasional sawtooth may be missing entirely, as shown in Fig.9. The precise relationship between the JWKB and quantal cross sections can only be understood by a careful study of the relevant JWKB and quantal phase shifts. Some of these phenomena have been pointed out previously by Vogt and Wannier[20a] and by Dalgarno, Mc Dowell, and Williams.[13] Similar sawteeth have also been noticed in calculations of JWKB spin-exchange cross sections.[20b]

In the classical approximation, the orbiting sawteeth do not occur, and only the smoothly varying mean is found. The rainbow undulations persist, however, and it is interesting to inquire how this comes about. The reason is easiest to see in terms of the expression for $S^{(n)}$ in terms of $\sigma(\chi)$, given by Eq.(3). The rainbow scattering produces a singularity and discontinuity in $\sigma(\chi)$ at χ_r in the classical approximation,[1,21] but $\sigma(\chi)$ is smooth in the orbiting region. This rainbow in $\sigma(\chi)$ can have a large or small effect on $S^{(n)}$ depending on the angle at which it occurs, because of the weighting factors $(1-\cos^n\chi)$.

At energies just above that for which classical orbiting ceases, the value of χ_r changes quite rapidly with E, and can change from a large multiple of π to a smaller multiple of π for a small change in E. The rainbow in $\sigma(\chi)$ thus shifts rapidly in angle as E is changed, and this augments $S^{(n)}$ if $(1-\cos^n\chi)$ is large but has little effect if $(1-\cos^n\chi)$ is small. The net result is an undulatory behavior in $S^{(n)}$ until the energy is high enough that χ_r becomes less than π and continues to decrease as E is increased, whereby the $(1-\cos^n\chi)$ factors quickly damp out the undulation. This undulatory behavior was noticed in the pioneering calculations of $S^{(n)}$ for the 12-6 potential by Hirschfelder, Bird, and Spotz,[22] but was incorrectly attributed by them to orbiting rather than to rainbows. It was later correctly interpreted by Dalgarno and Smith.[23]

The foregoing effects are illustrated in Fig. 9, which shows $S^{(1)}$ as a function of energy in the classical, JWKB, and quantal limits for $\Lambda^* = 1.0$. The difficulty with the JWKB orbiting sawteeth is that they become more numerous as Λ^* becomes smaller and classical behavior is supposedly approached more closely. Thus the cross sections must be evaluated at very small intervals of energy if the behavior is to be followed. If this is not done, one obtains points more or less at random on the sawteeth, and the appearance may be that of a random scattering of points about the classical curve. Worse still, if the points are calculated for a wide spacing of E, an entirely erroneous impression may be obtained of undulations of much longer wavelength.

The question therefore arises as to how to smooth out the sawteeth without undue labor. The best way would be to use quantal phase shifts where necessary and only to use JWKB phase shifts in regions of proper validity as shown in Fig. 2. This can still involve a great deal of numerical computation since there may be just as many quantal undulations as there are JWKB sawteeth. A much easier way would be to recognize that it is seldom necessary to follow the undulations precisely, except possibly for large Λ^* when the JWKB approximation is bad anyway, since the undulations are usually wiped out by subsequent integrations over the velocity distributions in the case of $S^{(n)}$, or by limited resolution or velocity selection in the case of S. This being the case, it is better to use the semiclassical approximation in which the summations over ℓ are replaced by integrations. But we have already seen that this leads exactly to the classical result in the case of the transport cross sections. This confirms our previous observation that it is seldom worthwhile to bother with the JWKB approximation to $S^{(n)}$: if the JWKB approximation is accurate, the classical calculation is both easier and more accurate; if the classical calculation is inaccurate so is the JWKB one.

From an examination of Fig. 9 it is evident that classical transport cross sections at orbiting energies are considerably in error for a gas with $\Lambda^*=1$. It might therefore appear that the transport properties of any light gas could not be accurately predicted by classical theory at orbiting

energies. This would suggest that classical theory might be inadequate for atomic hydrogen below about 10,000 ^{o}K (since $\epsilon \approx 4.7$ eV for the singlet state of H_2). Yet recent classical calculations of the viscosity of atomic hydrogen by Dalgarno and Smith[23] have agreed within one or two percent with exact quantal calculations by Buckingham and Fox[24] down to 100 ^{o}K, and semiclassical calculations of thermally averaged spin-exchange cross sections for atomic hydrogen by Smith[25] have been in good agreement with similar quantal calculations by Dalgarno and Henry[26] and by Buckingham and Fox[27] down to 10 ^{o}K. This apparent contradiction can nevertheless be explained in terms of the results already discussed.

There are two interaction potentials for atomic hydrogen corresponding to the $^{1}\Sigma_g$ and $^{3}\Sigma_u$ states of H_2. The triplet potential has $\epsilon \approx 0.0014$ eV and $\sigma \approx 5.7a_o$, so that $\Lambda^* \approx 3.6$. Although Λ^* is large, ϵ is so small that most thermal energies lie far above the orbiting region and quantum deviations are small. The singlet potential has $\epsilon \approx 4.7$ eV and $\sigma \approx 0.85\ a_o$, so that $\Lambda^* \approx 0.4$ and the classical approximation is accurate. The major error is thus the lack of the orbiting sawteeth for the singlet cross sections, but these are effectively eliminated by the subsequent thermal averaging and the final classical and quantal results are nearly equal.

Glory Effects

The effects of forward glory scattering are worth a few comments. Classically, glory scattering occurs at the point where the deflection curve χ crosses the b-axis, and quantally occurs at the point where δ_ℓ vs. ℓ has a maximum, as shown in Fig. 5. Here $\sigma(\chi)$ is infinite, but $\sigma(\chi) \sin \chi$ is finite.[1] The effect on the transport cross sections is simply to lower them slightly, because the weight factors $(1-\cos^n\chi)$ are all zero at $\chi = 0$. This is probably the reason that the small attractive part of the 12-6 potential had such an influence on $S^{(2)}$ at high energies, as was shown in Fig. 8: the effect of the attraction, even though it is weak, is to produce a forward glory which is absent for a purely repulsive potential. This lowering can also be easily understood from the formulae for $S^{(n)}$ in terms of the sums over δ_ℓ given by Eqs.(5) and (6). In the vicinity of the glory, δ_ℓ changes very slowly with ℓ, so that $(\delta_{\ell+n} - \delta_\ell)$ and hence $\sin^2(\delta_{\ell+n} - \delta_\ell)$ is nearly zero, and the phase shifts around the glory do not contribute much to $S^{(n)}$.

The effect of the glory on the total scattering cross section is much more dramatic. Because δ_ℓ is slowly varying, there is a whole set of terms in the summation for which $\sin^2 \delta_\ell$ is nearly the same. For other terms δ_ℓ varies more rapidly and hence $\sin^2 \delta_\ell$ oscillates. Whenever the value of δ_ℓ near the glory is near $\pi/2$, $\sin^2\delta_\ell$ takes on its maximum value

and there is a contribution to the cross section from the glory phases. Whenever δ_ℓ near the glory is π, $\sin^2\delta_\ell$ is small and there is no contribution to the cross section from the glory phases. Thus S vs. E undulates at low energies, as the values of the glory phases pass successively through $\pi/2$ and π. This undulatory behavior was first noticed by Bernstein,[4] who also pointed out that the number of undulations was related (semi-classically) to the number of bound states of the potential.[28] The phenomenon has since been observed experimentally and analysed in detail.[29] We need say nothing further about it except to remark that the orbiting undulations (or semiclassical sawteeth) will be superposed on the glory undulations. For small Λ^* this is an unimportant effect and can be removed by replacing the summation by an integration, or by just drawing a smooth curve through a set of calculated points. However, as Λ^* increases the glory undulations become fewer and the orbiting undulations become of comparable importance. Finally for large Λ^* there are no glory undulations at all, but promiment orbiting undulations. A little care is thus necessary in drawing conclusions about the number of bound states from the number of extrema in S vs. velocity. For instance, there are several low-velocity extrema in S for $\Lambda^* = 2.67$ (corresponding to He^4), but there is at most one bound state.[10,30] These extrema are in fact related to classical orbiting rather than to glory scattering. In actual practice there should be no real difficulty, since the location of the orbiting undulations, if they are present, can be predicted from

a knowledge of the orbiting line and its continuation, the rainbow scattering line.

Small-Angle Differential Cross Sections

As a final example we compare the differential cross section for a pure r^{-12} repulsive potential as calculated from the exact quantal phase shifts and from some recently derived[19] semiclassical approximations. The latter were given in two parts, one valid at very small angles and the other at larger angles where the scattering is nearly classical. For a potential varying as r^{-s}, the small angle result is

$$\sigma(\chi) = \left(\frac{kS}{4\pi}\right)^2 \left[1 + \tan^2\left(\frac{\pi}{s-1}\right)\right] \exp\left[-\frac{f(s)k^2S\chi^2}{8\pi}\right] , \quad (20)$$

where f(s) is a numerical constant equal to 1.078 for s=12. The nearly classical result is

$$\sigma(\chi) = \sigma_{c\ell}(\chi)\left[1 + (2kb\chi)^{-2} + \cdots\right] , \quad (21)$$

which does not claim to do more than supply an indication of the region where quantum deviations begin to be important. In particular, Eq.(21) will not exhibit any quantal oscillations, but will give only the mean value.

The numerical comparison is shown in Figs. 10 and 11, which were calculated with the potential

$$\varphi = 4\epsilon(\sigma/r)^{12} , \quad (22)$$

using an energy $E/\epsilon = 45$ and de Boer parameters of $\Lambda^* = 0.50$ and 2.67. The quantum oscillations at larger angles, due to the Legendre polynomials in the expression for $\sigma(\chi)$, are indeed not reproduced by Eq.(21). The small-angle result of Eq.(20), however, is in remarkably good agreement with the exact results out to much larger angles than originally claimed,[19] provided that the exact value of the total cross section S is used in Eq.(20). The agreement is not so good if an approximate value of S based on the Massey-Mohr[31] approximation to the JWKB phases is used. This approximate S is given for s=12 by the expression

$$S = F_{12} \, (4\epsilon\sigma^{12}/\hbar v)^{2/11} \quad , \tag{23}$$

where[19] $F_{12} = 6.584$. The Massey-Mohr approximation is the limiting form taken by the JWKB formula for small phase shifts; in the cases shown in Figs. 10 and 11, the phase shifts which contribute most strongly to S are not so small (of the order of 0.2 rad), and consequently Eq.(23) is not very accurate.

It is also remarkable how closely the Massey-Mohr value of the critical angle χ_c describes the location of the angle where the quantal $\sigma(\chi)$ crosses the nearly classical $\sigma(\chi)$ for the second time, after which it oscillates rather symmetrically about the classical curve. The value of the critical angle is

$$\chi_c = \pi/(kr_o) \approx \pi/(k\sigma), \tag{24}$$

where r_o is the classical distance of closest approach for scattering through the angle χ_c.

V. CONCLUSIONS

Although our numerical calculations have been restricted to a particular potential model, we believe the following conclusions are fairly general:

(1) The JWKB approximation for the scattering phase shifts always fails in a certain region whose extent depends on the value of the de Boer parameter Λ^*. The boundaries of this region can be predicted on the basis of a small number of calculations.

(2) The JWKB approximation is essentially useless for the calculation of transport cross sections. For low energies or large Λ^* it is inaccurate, and where it is accurate the purely classical approximation gives the same averaged cross sections and is easier to use.

(3) The JWKB approximation is useful for the calculation of total scattering cross sections, for which the classical approximation always fails, but it is accurate only for high energies or for small values of Λ^*.

(4) The analogue of classical orbiting collisions causes several peculiar features to appear in the cross sections, and this behavior must be taken into account in detailed comparisons of

experiment and theory.

(5) The differential cross section behaves very nearly as exp $(-c\chi^2)$ out to the Massey-Mohr critical angle χ_c, and then oscillates about a nearly classical mean value.

ACKNOWLEDGMENT

We thank the University of Maryland Computer Science Center for their kindness in making extra IBM 7090 time available, and Professor W. M. Benesch for pointing out the advantages of Numerov's method of integration.

APPENDIX: CALCULATION OF QUANTAL PHASE SHIFTS

A number of effective methods for calculating quantal phase shifts have been described in the literature.[2,10,32] In the present work, the radial wave equation in the form

$$\frac{d^2G_\ell(\rho)}{d\rho^2} + \left[\left(\frac{2\pi}{\Lambda^*}\right)^2 \frac{E}{\epsilon} - \frac{\ell(\ell+1)}{\rho^2} - \left(\frac{2\pi}{\Lambda^*}\right)^2 \left(\frac{4}{\rho^{12}} - \frac{4}{\rho^6}\right)\right] G_\ell(\rho) = 0, \tag{25}$$

where $\rho = r/\sigma$, was integrated using Numerov's procedure.[33] This is based on the relation

$$y_n = \frac{2y_{n-1} - y_{n-2} + (h^2/12)\left[y_{n-2}\, f(\rho_{n-2}) + 10y_{n-1}\, f(\rho_{n-1})\right]}{1-(h^2/12) f(\rho_n)}, \tag{26}$$

where $y_n = G_\ell(\rho_n)$, $h = \rho_n - \rho_{n-1}$, and

$$f(\rho) = \left(\frac{2\pi}{\Lambda^*}\right)^2 \left(\frac{4}{\rho^{12}} - \frac{4}{\rho^6}\right) + \frac{\ell(\ell+1)}{\rho^2} - \left(\frac{2\pi}{\Lambda^*}\right)^2 \frac{E}{\epsilon} \quad . \tag{27}$$

It can be shown[33] that the first-order error per cycle for the quadrature is $h^6\ y^{VI}/240$.

The program performed in the following way. The radial equation was integrated outwards from a point where the solution was essentially zero. In practice it was found that the exact choice of starting values was not critical; the two initial values were usually chosen to be equal and of the order of 10^{-6}. The integration was continued until the potential was less than 10^{-6} the total energy, that is until

$$\left| \frac{4}{\rho^{12}} - \frac{4}{\rho^6} \right| < 10^{-6} \frac{E}{\epsilon} \quad . \tag{28}$$

A check was then commenced for the next change in sign of the solution $G_\ell(\rho)$. When this occurred, the integration was carried out for two more steps and the position of the zero found by interpolation.

It is well known that the solution of Eq.(25) when the potential is zero is of the form

$$G_\ell(\rho) = A\rho^{\frac{1}{2}}\ J_{\ell+\frac{1}{2}}\ (k^*\rho) + B\rho^{\frac{1}{2}}\ J_{-\ell-\frac{1}{2}}\ (k^*\rho), \tag{29}$$

where $k^* = k\sigma$, and that the phase shift δ_ℓ is given by

$$\delta_\ell = \arctan\left[(-1)^\ell B/A\right]. \tag{30}$$

If ρ_o is the position of the last recorded zero of $G_\ell(\rho)$, it follows immediately that

$$\delta_\ell = \arctan\left[(-1)^\ell J_{\ell+\frac{1}{2}}(k^*\rho_o) / J_{-\ell-\frac{1}{2}}(k^*\rho_o)\right]. \tag{31}$$

The Bessel functions were calculated from a recursion relation, with $J_{\frac{1}{2}}$ and $J_{-\frac{1}{2}}$ as starting points.

The program was started with $\underline{\ell}=0$, and the value of $\underline{\ell}$ was increased by 1 after each phase shift was found. This was continued until four successive phase shifts were less than 0.001. The program then calculated the cross sections S, $S^{(1)}$, $S^{(2)}$ (even $\underline{\ell}$), $S^{(2)}$ (odd $\underline{\ell}$), and $S^{(3)}$. An option of calculating the differential cross sections at specified angles was also provided. Another energy could then be read in and the whole calculation repeated.

It has been previously noted[10,32] that phase shifts calculated by procedures similar to the foregoing are slightly in error because of the residual effect of the attractive tail of the potential. A small correction was therefore made to the calculated phase shifts, based on using the JWKB approximation to continue the solution $G_\ell(\rho)$ beyond its last recorded zero at ρ_o. This correction had the form

$$\delta_\ell(\text{true}) = \delta_\ell(\text{apparent}) + \Delta\delta_\ell, \tag{32}$$

where δ_ℓ(apparent) was the value from Eq.(31), and

$$\Delta\delta_\ell = k^* \int_{\rho_o}^{\infty} \left\{ \left[1 - \left(\frac{2\pi}{\Lambda^*} \right)^2 \frac{\varphi}{\epsilon k^{*2}} - \frac{\ell(\ell+1)}{(k^*\rho)^2} \right]^{\frac{1}{2}} - \left[1 - \frac{\ell(\ell+1)}{(k^*\rho)^2} \right]^{\frac{1}{2}} \right\} d\rho \ . \qquad (33)$$

At large separations, φ for the 12-6 potential can be approximated by $-4\epsilon/\rho^6$, and Eq.(33) becomes, after expansion of the integrands,[10,32]

$$\Delta\delta_\ell \approx \frac{2}{5k^*\rho_o^5} \left(\frac{2\pi}{\Lambda^*} \right)^2 \left[1 + \frac{5\ell(\ell+1)}{14(k^*\rho_o)^2} + \cdots \right] \ . \qquad (34)$$

In practice this correction was always less than 0.0001 rad.

Very accurate phase shifts for the Lennard-Jones (12-6) potential have been obtained for $\Lambda^* = 3.08$ and 2.67 (corresponding to He^3 and He^4).[10] These were later used by Keller[34] to calculate the viscosity cross sections $S^{(2)}$. Comparison of our calculated δ_ℓ with Keller's tables showed very close agreement, the discrepancy between the two calculations being always less than 0.005 rad. A comparison of our calculated $S^{(2)}$ with these tables also showed close agreement, the largest discrepancy being of the order of 0.2%.

It is difficult to estimate the time required to calculate a single phase shift by the present program, but a mean time, as determined on a sample of 10,000 phases, is about 0.5 sec on an IBM 7090.

FIGURE CAPTIONS

Fig. 1 - Phase shifts as a function of energy for the Lennard-Jones (12-6) potential with $\Lambda^* = 1.0$, showing the failure of the semiclassical JWKB results (broken curves) as compared with the exact quantal results (solid curves). The vertical arrows mark the classical orbiting energies. An apparent case of resonant barrier-tunneling is seen for $\ell=5$.

Fig. 2 - Regions in which the JWKB and exact quantal phase shifts differ by more than 0.05 radian for a 12-6 potential are exhibited as loops in the energy-angular momentum plane. The dashed curve shows where classical orbiting and rainbow scattering occur, the black dot marking the transition point from one to the other.

Fig. 3 - Effective potential energy curves, with ranges of E/ϵ indicated for which the JWKB phases are of unsatisfactory accuracy. Two curves are shown, one for which classical orbiting occurs, and one for which it cannot occur. These have centrifugal terms (or angular momenta) corresponding to $(b/\sigma)(E/\epsilon)^{\frac{1}{2}} = 1.3$ and 1.7, respectively.

Fig. 4 - Plot of E/ϵ vs. $(\Lambda^*)^2$ for the high-energy edges of the regions shown in Fig. 2. The upper line corresponds to the maximum value of E/ϵ for a given value of Λ^*, and the lower line corresponds to the value of E/ϵ for given Λ^* and angular momentum $(b/\sigma)(E/\epsilon)^{\frac{1}{2}} = 1.0$.

Fig. 5 - Schematic diagram of the JWKB phase shift and the corresponding classical deflection angle, showing the behavior around orbiting and a forward glory. The correct quantal phase shift is indicated by the dashed curve. (The results shown actually correspond approximately to $E/\epsilon = 0.4$ and $\Lambda^* = 1.0$.)

Fig. 6 - Percentage deviations of the classical (solid curves) and JWKB (dashed curves) diffusion cross sections $S^{(1)}$ from the correct quantal results, with $\Delta S^{(1)} = S^{(1)}(\text{approx.}) - S^{(1)}(\text{quantal})$.

Fig. 7 - Percentage deviations of the JWKB total scattering cross sections S from the correct quantal results, with $\Delta S = S(\text{approx.}) - S(\text{quantal})$.

Fig. 8 - Viscosity cross section $S^{(2)}$ for He^4 as calculated classically and quantally for the 12-6 potential, and quantally for the inverse 12th power repulsive potential. The originally conjectured connection between high and low energy results is shown as a dashed curve (de Boer and Bird). For He^4 the quantal summations run over only even values of $\underline{\ell}$.

Fig. 9 - Classical, JWKB, and quantal diffusion cross sections $S^{(1)}$ for $\Lambda^* = 1$, showing orbiting sawteeth and undulations as discussed in the text.

Fig. 10 - Differential scattering cross section for an inverse 12th power repulsive potential, with $E/\epsilon = 45$ and $\Lambda^* = 0.50$. Curves A and B are the small-angle approximation of Eq.(20), curve A being calculated with the exact value of S and curve B with an approximate value of S from Eq.(23).

Fig. 11 - Differential scattering cross sections as in Fig. 10, but with $\Lambda^* = 2.67$. The classical curves are identical in the two figures, but the scales are shifted.

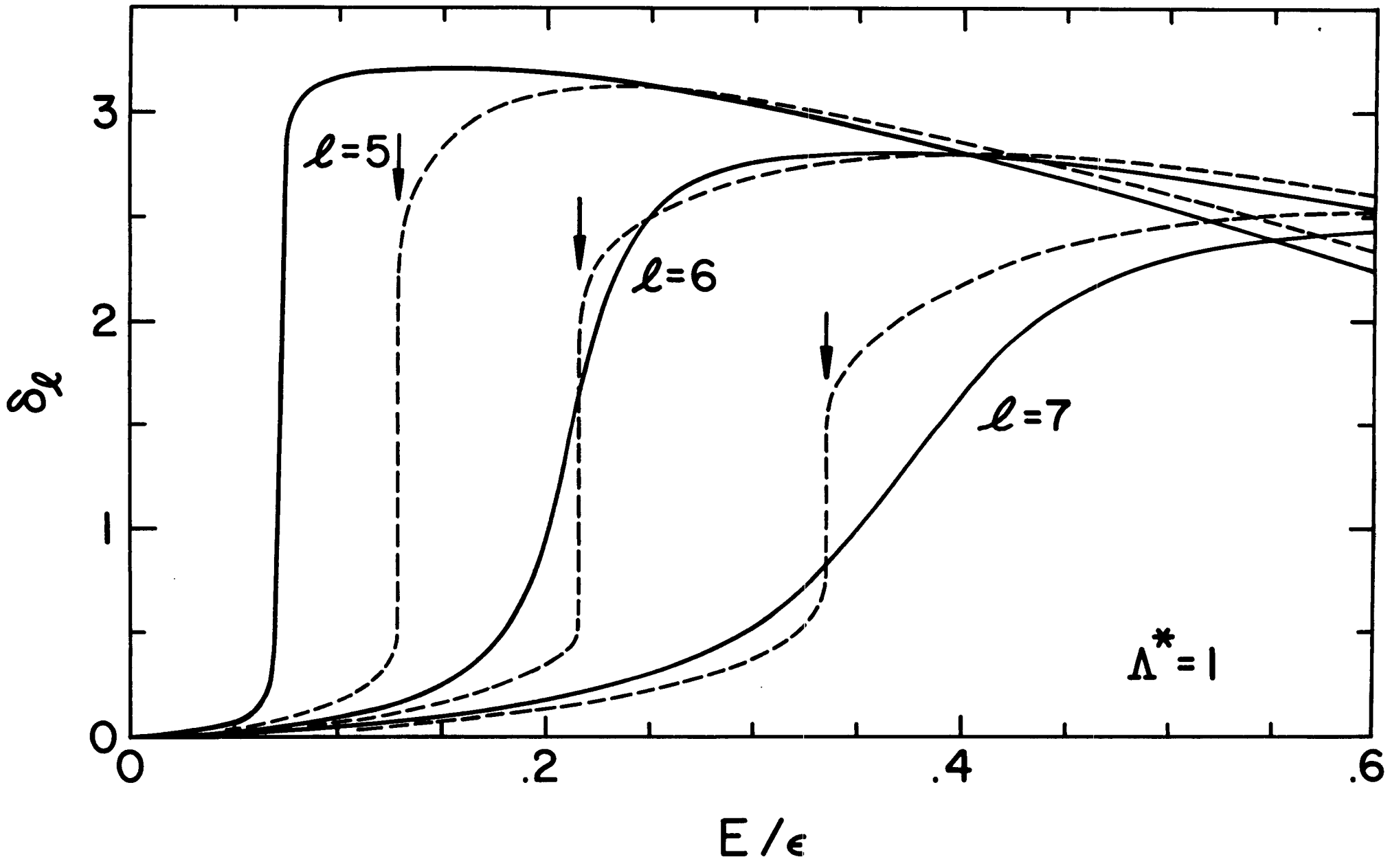
3
2
1
0
0
.2
.4
.6
δℓ
E/ϵ
ℓ=5
ℓ=6
ℓ=7
Λ*=1

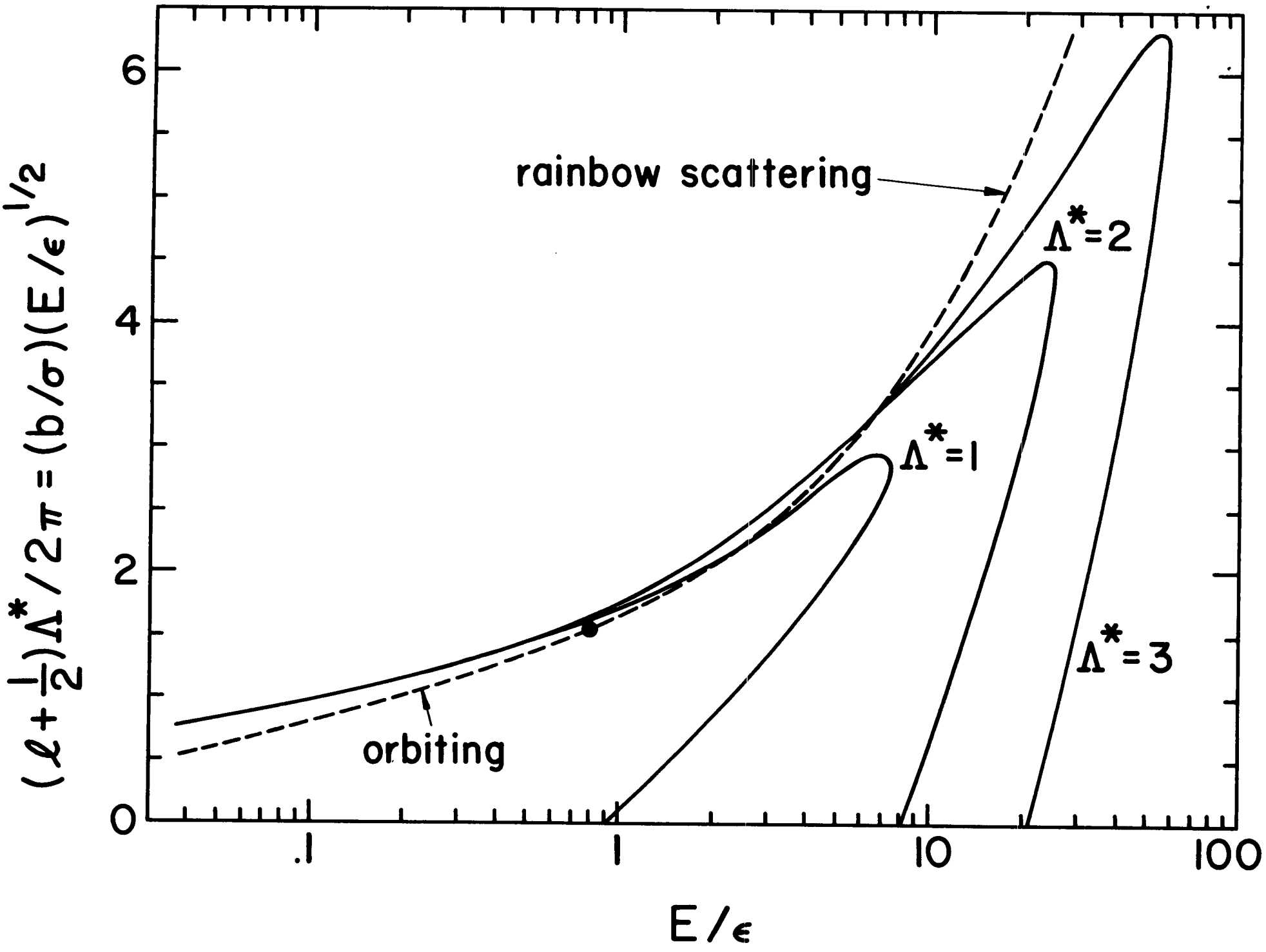
rainbow scattering
Λ*=2
Λ*=1
Λ*=3
orbiting
6
4
2
0
.1
1
10
100
$(\ell+\frac{1}{2})\Lambda^*/2\pi = (b/\sigma)(E/\epsilon)^{1/2}$
E/ϵ

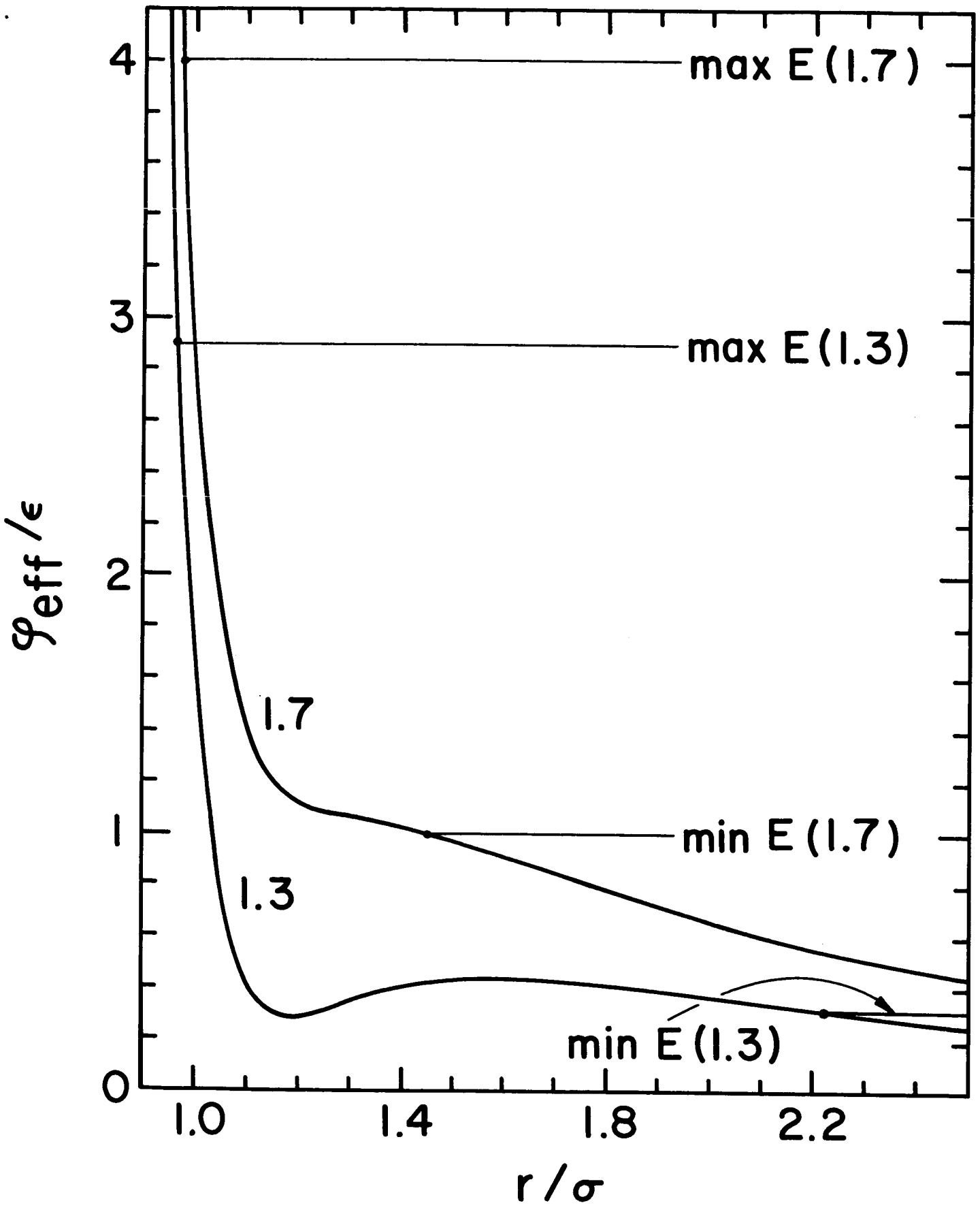
max E (1.7)
max E (1.3)
1.7
1.3
min E (1.7)
min E (1.3)
4
3
2
1
0
1.0
1.4
1.8
2.2
φ_{eff}/ϵ
r/σ

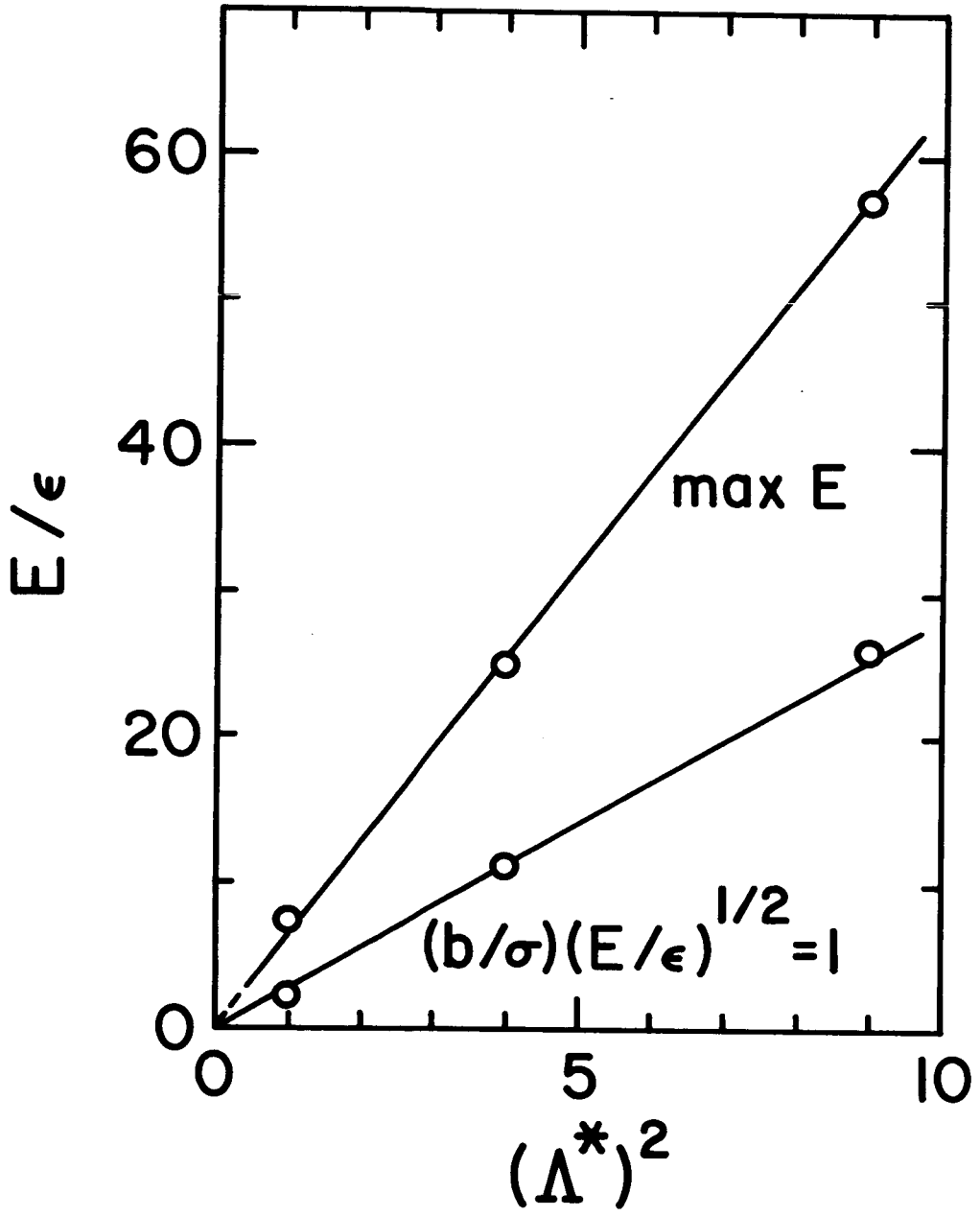
60
40
20
0
E/ε
max E
(b/σ)(E/ε)^1/2=1
0
5
10
(Λ*)^2

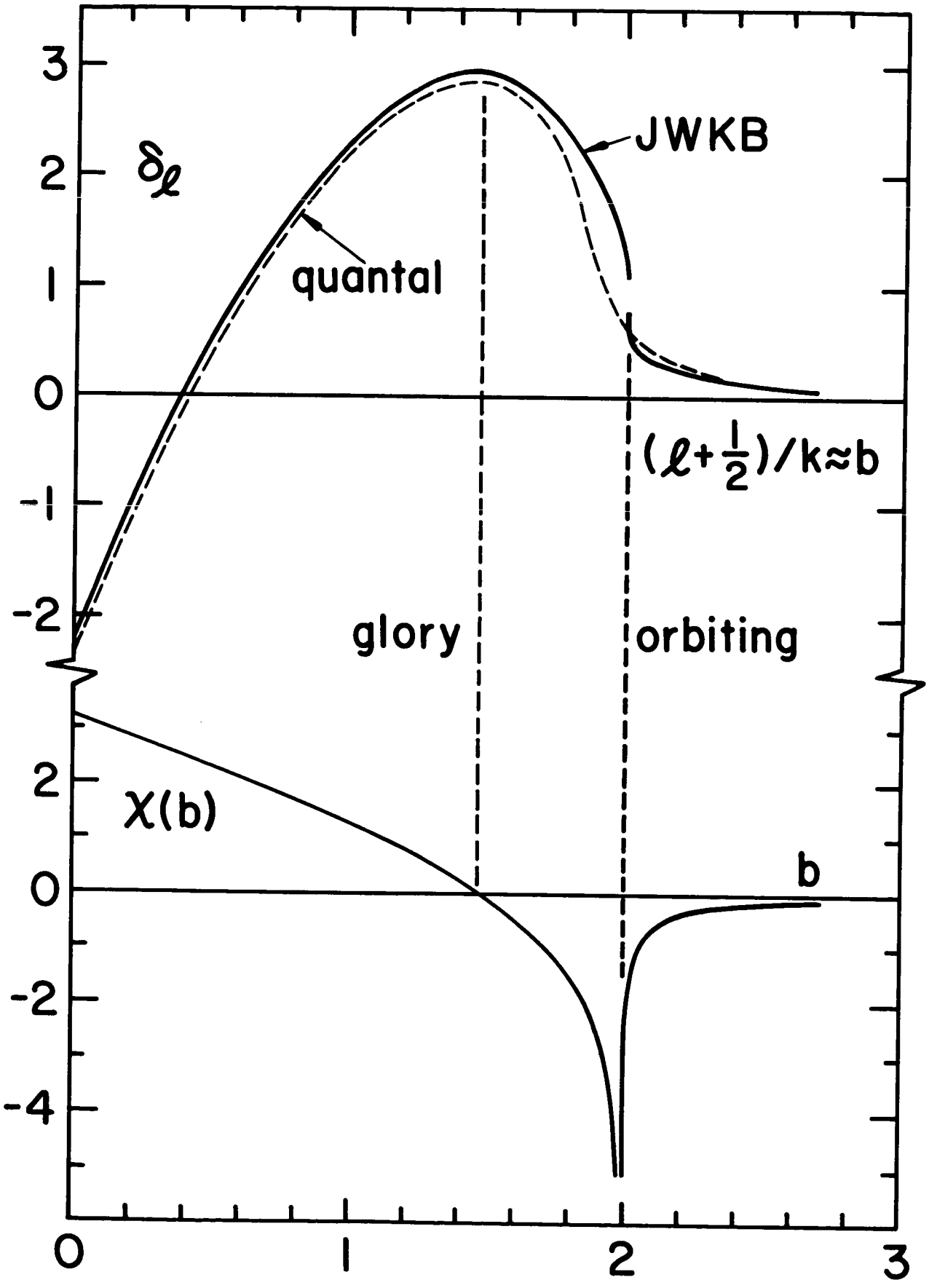
3
2
1
0
-1
-2
δ_ℓ
JWKB
quantal
$(\ell+\frac{1}{2})/k \approx b$
glory
orbiting
2
0
-2
-4
$\chi(b)$
b
0
1
2
3

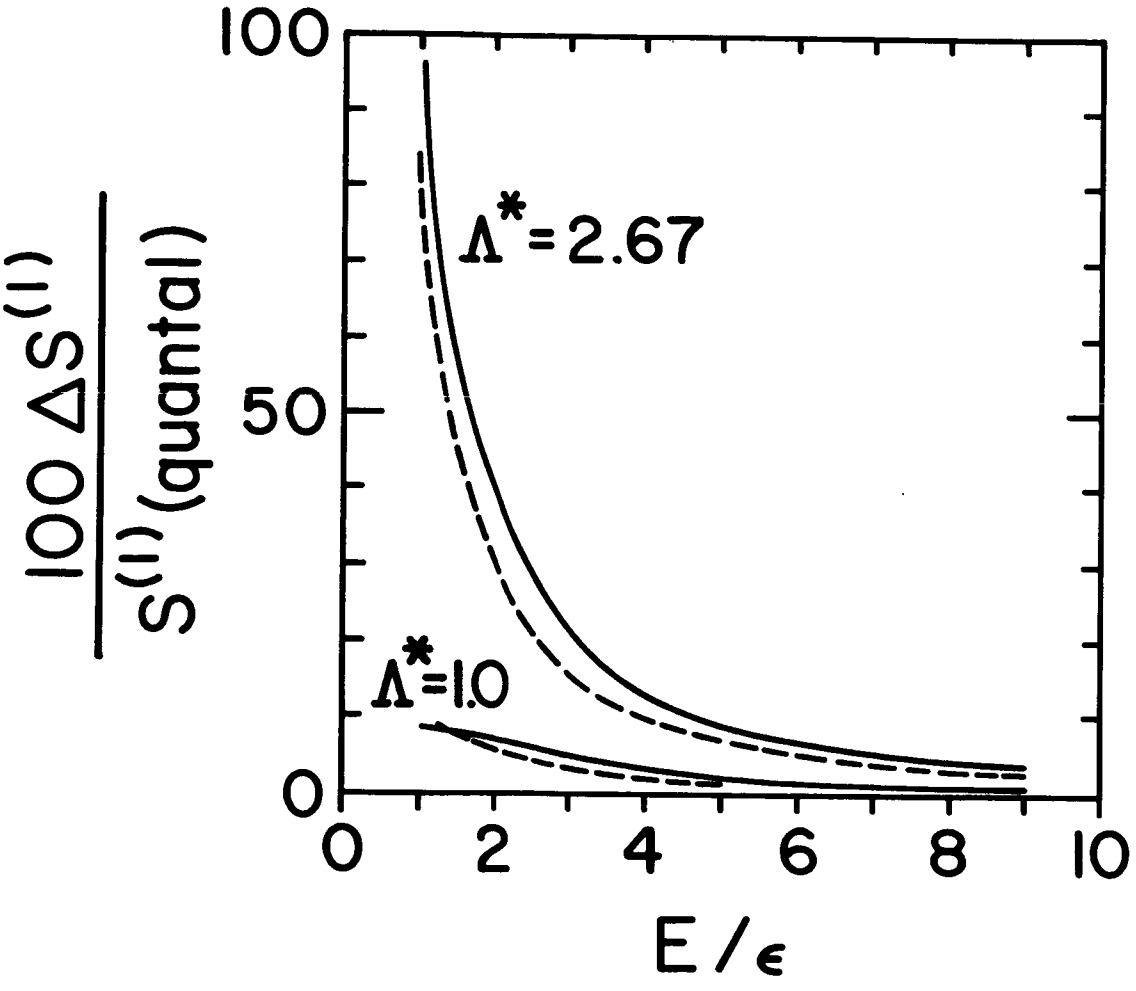
100
50
0
0
2
4
6
8
10
$\frac{100\,\Delta S^{(1)}}{S^{(1)}(\text{quantal})}$
$\Lambda^* = 2.67$
$\Lambda^* = 1.0$
E/ϵ

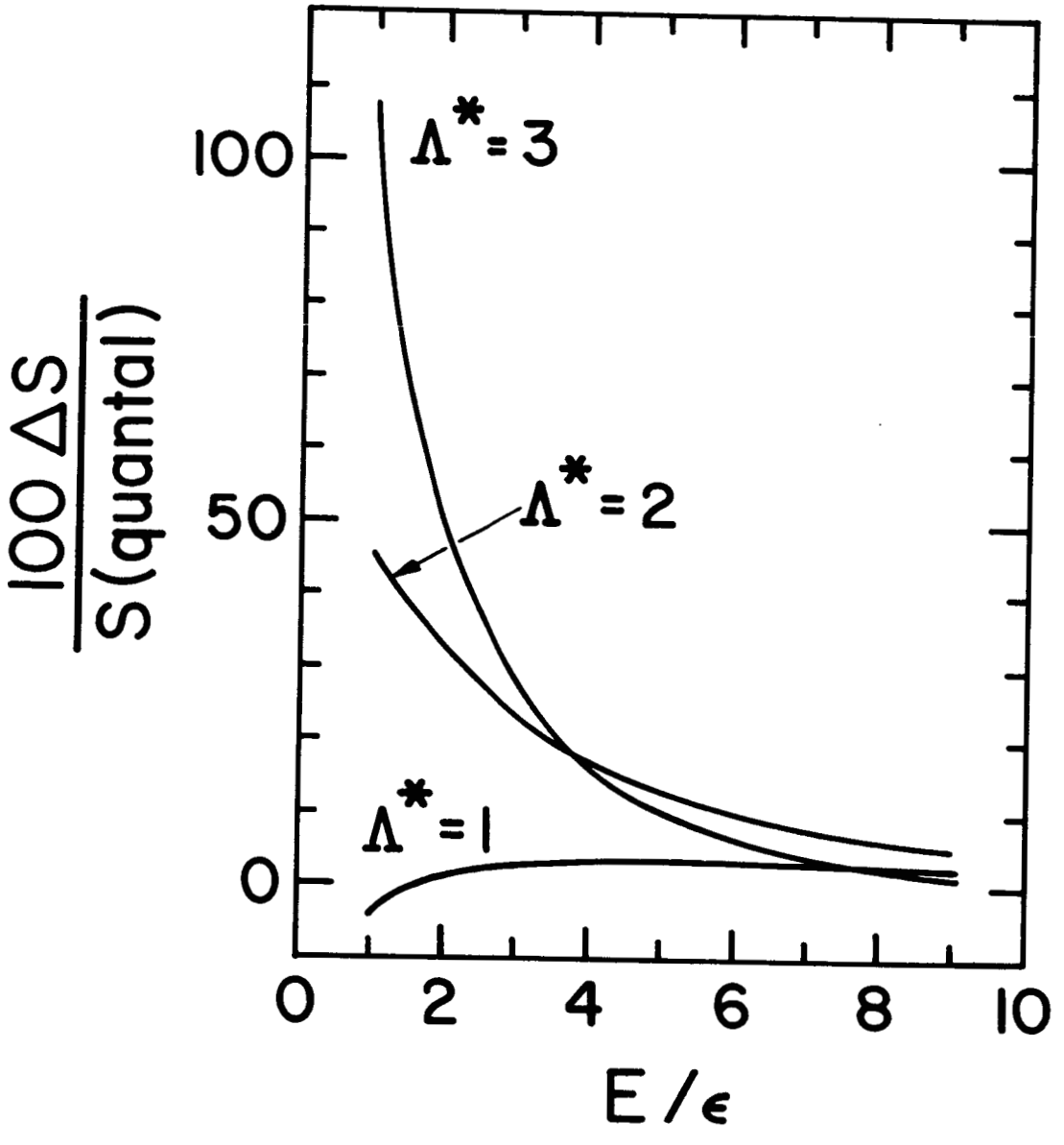
100 ΔS / S(quantal)
100
50
0
Λ* = 3
Λ* = 2
Λ* = 1
0
2
4
6
8
10
E / ϵ

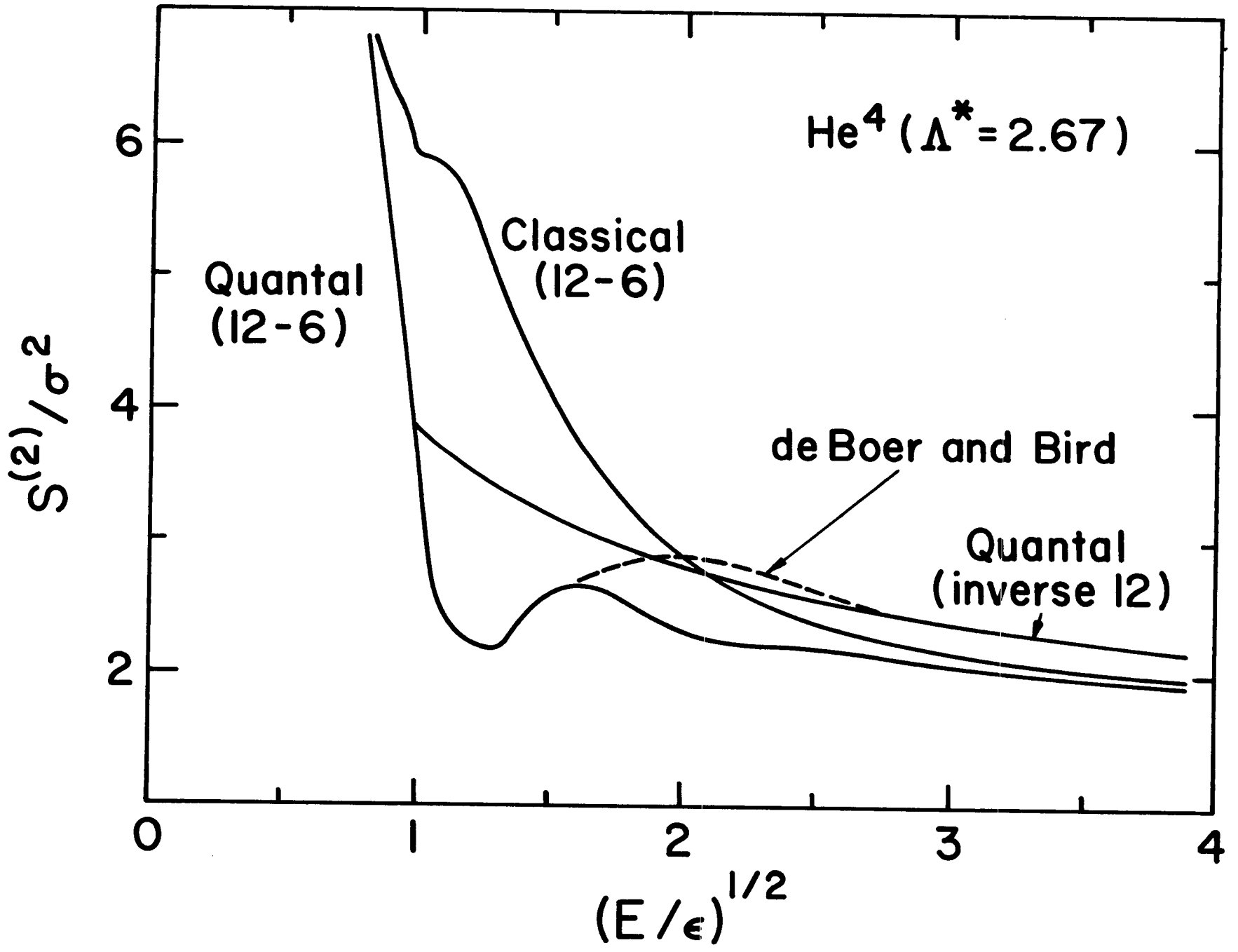
He^4 ($\Lambda^* = 2.67$)
Classical (12-6)
Quantal (12-6)
de Boer and Bird
Quantal (inverse 12)
$S^{(2)}/\sigma^2$
$(E/\epsilon)^{1/2}$
0
1
2
3
4
2
4
6

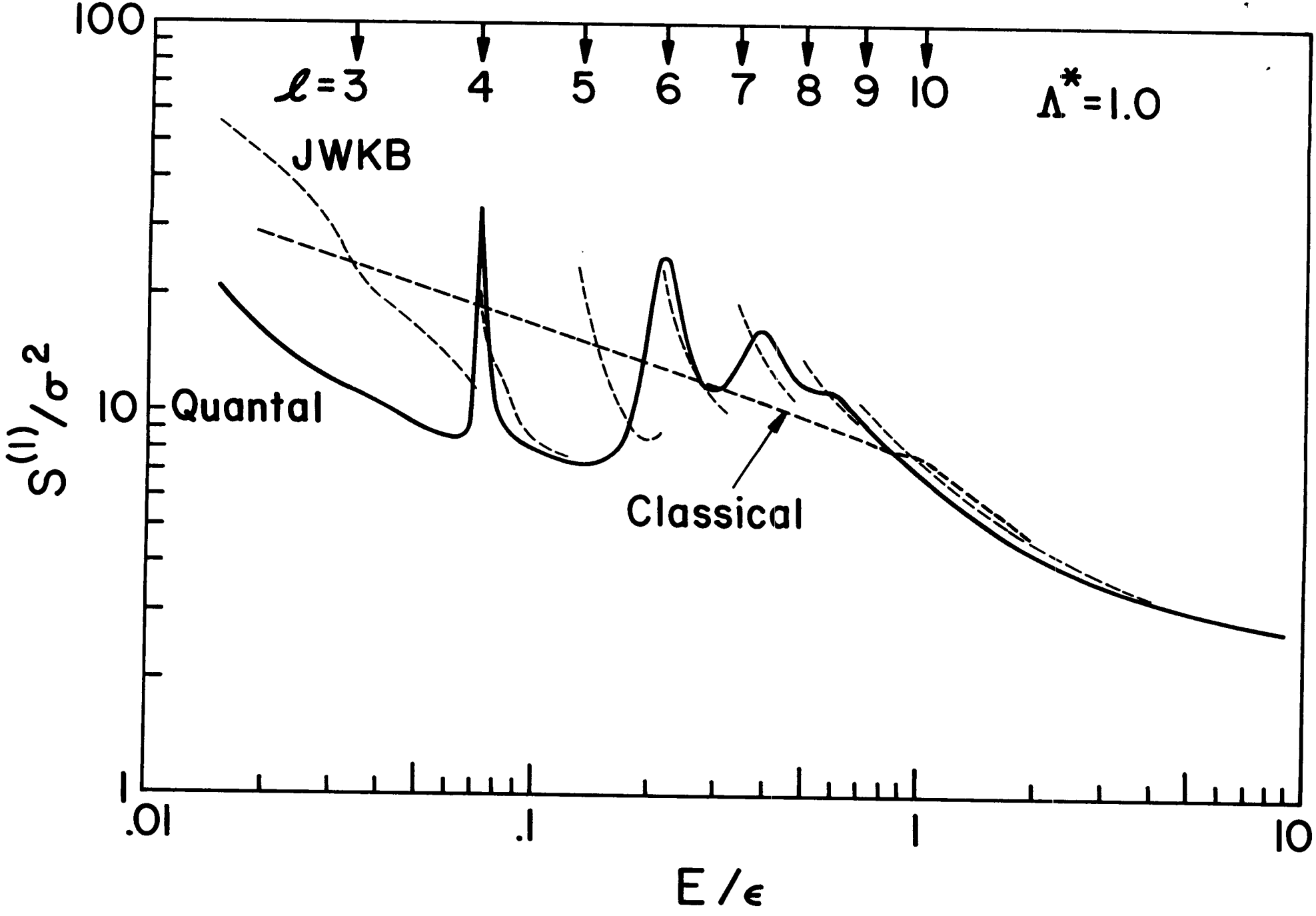
100
10
1
.01
.1
1
10
ℓ=3
4
5
6
7
8
9
10
Λ*=1.0
JWKB
Quantal
Classical
S(1)/σ2
E/ε

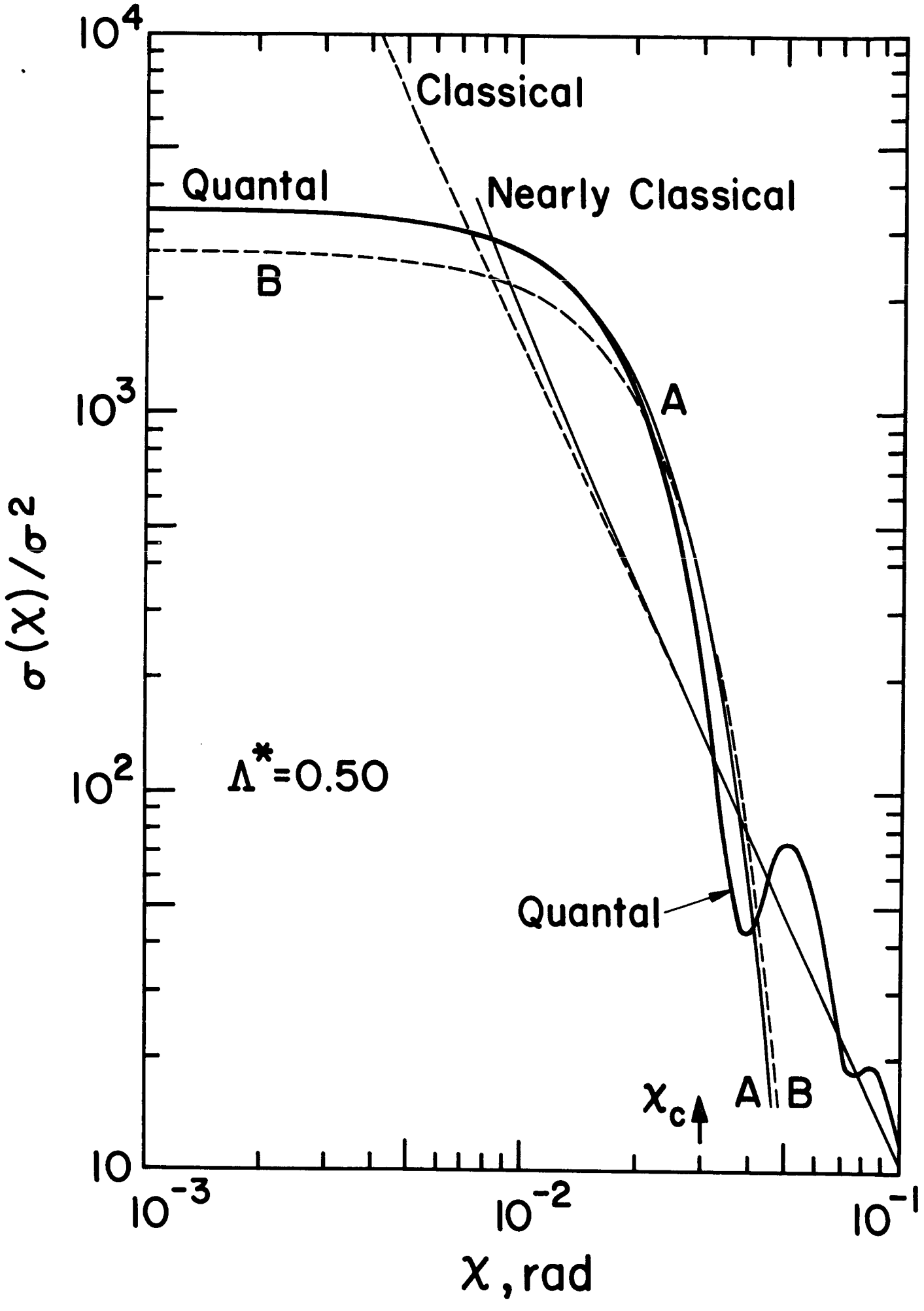
Classical
Quantal
Nearly Classical
B
A
Λ^*=0.50
Quantal
χ_c
A
B
10^4
10^3
10^2
10
10^{-3}
10^{-2}
10^{-1}
$\sigma(\chi)/\sigma^2$
χ, rad

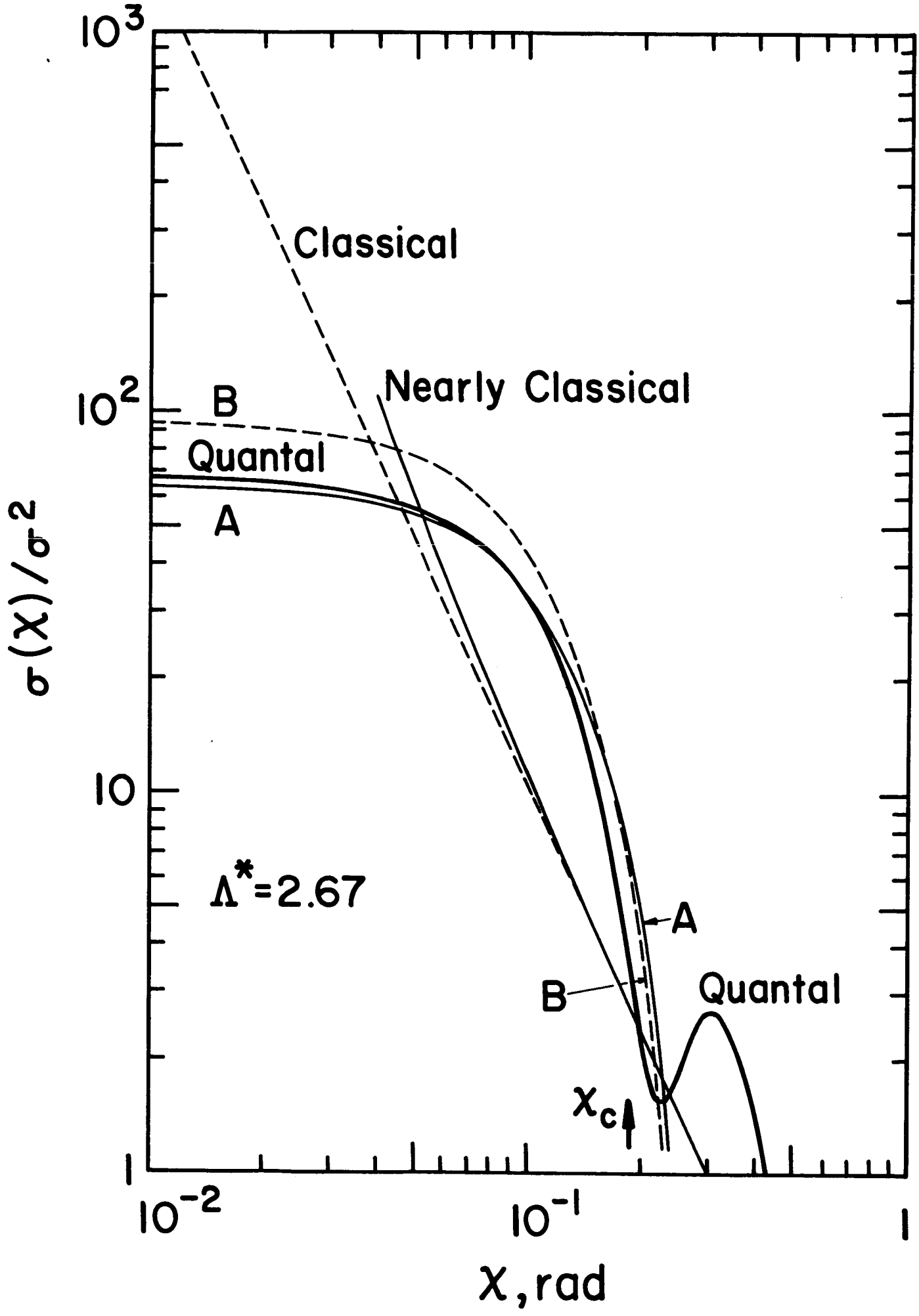
10^3
10^2
10
1
10^{-2}
10^{-1}
1
Classical
Nearly Classical
B
Quantal
A
$\sigma(\chi)/\sigma^2$
$\Lambda^*=2.67$
A
B
Quantal
χ_c
χ, rad

REFERENCES

1 (a) K. W. Ford and J. A. Wheeler, Ann. Phys. (N.Y.) 7, 259 (1959); (b) ibid. 7, 287(1959).

2 R. B. Bernstein, J. Chem. Phys. 33, 795(1960); 36, 1403(1962).

3 R. P. Marchi and C. R. Mueller, J. Chem. Phys. 36, 1100(1962); 38, 740(1963).

4 R. B. Bernstein, J. Chem. Phys. 34, 361(1961).

5 C. R. Mueller and J. W. Brackett, J. Chem. Phys. 40, 654(1964).

6 J. O. Hirschfelder, C. F. Curtiss, and R. B. Bird, Molecular Theory of Gases and Liquids (John Wiley and Sons, Inc., New York, 1954), Chap. 10.

7 R. A. Buckingham and A. Dalgarno, Proc. Roy. Soc. (London) A213, 506(1952); C. F. Curtiss and R. S. Powers, Jr., J. Chem. Phys. 40, 2145(1964); see also S. Choi and J. Ross, J. Chem. Phys. 40, 2151(1964).

8 F. J. Smith and R. J. Munn (to be published); F. J. Smith, Physica 30, 497(1964).

9 L. I. Schiff, Quantum Mechanics (Mc Graw-Hill Book Company, Inc., New York, 1949), pp. 92-95.

10 J. E. Kilpatrick, W. E. Keller, E. F. Hammel, and N. Metropolis, Phys. Rev. 94, 1103(1954), and earlier references.

11 S. Choi and J. Ross, Proc. Natl. Acad. Sci. 48, 803(1962).

12 S. Geltman, Phys. Rev. 90, 808(1953).

13 A. Dalgarno, M.R.C. McDowell, and A. Williams, Phil. Trans. Roy. Soc. (London) A250, 411(1958).

[14] F. J. Smith, J. T. Vanderslice, and E. A. Mason (to be published).

[15] E. A. Mason and H. W. Schamp, Jr., Ann. Phys. (N.Y.) 4, 233(1958).

[16] H. T. Wood and C. F. Curtiss, J. Chem. Phys. (to be published).

[17] J. de Boer, Physica 10, 348(1943).

[18] J. de Boer and R. B. Bird, Physica 20, 185(1954).

[19] E. A. Mason, J. T. Vanderslice, and C.J.G. Raw, J. Chem. Phys. 40, 2153(1964).

[20] (a) E. Vogt and G. H. Wannier, Phys. Rev. 95, 1190(1954);
(b) F. J. Smith, Thesis, Queen's University of Belfast (1962);
A. E. Glassgold and S. A. Lebedeff, Ann. Phys. (N.Y.) 28, 181(1964).

[21] E. A. Mason, J. Chem. Phys. 26, 667(1957).

[22] J. O. Hirschfelder, R. B. Bird, and E. L. Spotz, J. Chem. Phys. 16, 968(1948).

[23] A. Dalgarno and F. J. Smith, Proc. Roy. Soc. (London) A267, 417(1962).

[24] R. A. Buckingham and J. W. Fox, Proc. Roy. Soc. (London) A267, 102(1962).

[25] F. J. Smith, Planet. Space Sci. 11, 1126(1963).

[26] A. Dalgarno and R.J.W. Henry, Proc. Phys. Soc. (London) 83, 157(1964).

[27] R. A. Buckingham and J. W. Fox, (private communication).

[28] R. B. Bernstein, J. Chem. Phys. 37, 1880(1962); 38, 2507(1963).

29 E. W. Rothe, P. K. Rol, S. M. Trujillo, and R. H. Neynaber, Phys. Rev. 128, 659(1962); P. K. Rol and E. W. Rothe, Phys. Rev. Letters 9, 494(1962); E. W. Rothe, P. K. Rol, and R. B. Bernstein, Phys. Rev. 130, 2333(1963); E. W. Rothe, R. H. Neynaber, B. W. Scott, S. M. Trujillo, and P. K. Rol, J. Chem. Phys. 39, 493(1963).

30 J. E. Kilpatrick and M. F. Kilpatrick, J. Chem. Phys. 19, 930(1951); J. E. Kilpatrick, W. E. Keller, and E. F. Hammel, Phys. Rev. 97, 9(1955); T. Kihara, Y. Midzuno, and T. Shizume, J. Phys. Soc. Japan 10, 249(1955).

31 H.S.W. Massey and C.B.O. Mohr, Proc. Roy. Soc. (London) A141, 434(1933); A144, 188(1934).

32 R. A. Buckingham, A. R. Davies, and D. C. Gilles, Proc. Phys. Soc. (London) 71, 457(1958); R. A. Buckingham and J. W. Fox, Proc. Roy. Soc. (London) A267, 102(1962).

33 K. S. Kunz, Numerical Analysis (Mc Graw-Hill Book Company, Inc., New York, 1957), pp. 204-206.

34 W. E. Keller, Phys. Rev. 105, 41(1957). Detailed tabulations of these results are available from the Library of Congress Documentation Institute as ADI 5064.